doi:10.3788/gzxb20184704.0431002

Tm^{3+}掺杂 $Na_5Lu_9F_{32}$单晶体的 1.8 μm 优化发射性能研究

盛启国[1],夏海平[1],汤庆阳[1],何仕楠[1],章践立[1],陈宝玖[2]
(1 宁波大学 光电子功能材料重点实验室,浙江 宁波 315211)
(2 大连海事大学 物理系,辽宁 大连 116026)

摘 要:采用改进过的布里奇曼法成功地生长了Tm^{3+}离子浓度从0.5~4 mol%变化的高质量$Na_5Lu_9F_{32}$单晶.在790 nm LD激发下,研究了不同Tm^{3+}掺杂晶体在1.86 μm波段的荧光发射性能、衰减曲线以及Tm^{3+}离子之间的能量传递过程.当Tm^{3+}离子掺杂浓度增加到~1.95 mol%时,晶体在1.86 μm处的荧光发射强度达到最大.然后,随着Tm^{3+}离子浓度进一步的增大,发射强度迅速下降.然而,Tm^{3+}离子在$^3F_4$能级处的荧光寿命随着Tm^{3+}掺杂浓度从0.5增加到4 mol%,逐渐降低.同时计算了1.86 μm处最大的受激发射截面为0.80×10^{-20} cm^2.Tm^{3+}离子的浓度猝灭效应和离子之间的交叉弛豫能量传递过程是造成1.86 μm荧光发射变化的主要原因.

关键词:Tm^{3+}离子;$Na_5Lu_9F_{32}$单晶;1.8 μm发射;布里奇曼法;交叉弛豫过程
中图分类号:O782; O734 **文献标识码**:A **文章编号**:1004-4213(2018)04-0431002-6

Optimizational 1.8 μm Emission of $Na_5Lu_9F_{32}$ Single Crystal Doped with Tm^{3+} Ions

SHENG Qi-guo[1], XIA Hai-ping[1], TANG Qing-yang[1], HE Shi-nan[1], ZHANG Jian-li[1], CHEN Bao-jiu[2]
(1 *Key Laboratory of Photoelectronic Materials, Ningbo University, Ningbo, Zhejiang* 315211, *China*)
(2 *Department of Physics, Dalian Maritime University, Dalian, Liaoning* 116026, *China*)

Abstract: The high quality $Na_5Lu_9F_{32}$ single crystals with different Tm^{3+} concentrations ranging from 0.5 to 4 mol% were grown successfully by an improved Bridgman method. The fluorescence spectra and decay curves at 1.86 μm were measured under the excitation of 790 nm LD to study the luminescent properties of the crystals and the energy transfer process between Tm^{3+} ions. The 1.86 μm emission intensity gradually increases to the maximum value when the Tm^{3+} concentration increases to around 1.95 mol%. Nevertheless, it decreases fleetly with the Tm^{3+} concentration further increase from 2.0 mol% to 4.0 mol%. The maximum stimulated emission cross section at 1.86 μm is also calculated to 0.80×10^{-20} cm^2. The 1.86 μm fluorescence lifetime of Tm^{3+} : $^3F_4$ level decreases with the increase of Tm^{3+} doping concentration. The concentration quenching effect of Tm^{3+} ions and the cross relaxation energy transfer process between Tm^{3+} ions are mainly in charge of the variety of the 1.86 μm emission.

Key words: Tm^{3+} ion; $Na_5Lu_9F_{32}$ single crystal; 1.8 μm emission; Bridgman method; Cross relaxation process
OCIS Codes: 310.5696; 310.6860; 140.3380; 160.4760; 260.1180; 260.2160; 300.6340

Foundation item: The National Natural Science Foundation of China (Nos.51772159, 51472125), the Natural Science Foundation of Zhejiang Province (No. LZ17E020001), and K. C. Wong Magna Fund in Ningbo University

First author: SHENG Qi-guo(1991—), male, M. S. degree candidate, mainly focuses on mid-infrared laser material scientific analysis, and photoelectronic function singly crystal growth. Emai:aiqgsheng@163.com
Contact author: XIA Hai-ping(1967—), male, professor, Ph. D. degree, mainly focuses on optical material synthesis, functional crystal growth research, laser optics, etc. Email:hpxcm@nbu.edu.cn

Received: Oct.8, 2017; **Accepted**: Dec.14, 2017

0 Introduction

The synthesis of Tm^{3+} doped materials and development of 2.0 μm mid-infrared solid state lasers are inducing intense interest because of their potential applications in material processing, distance measurement, laser medical and remote sensing[1-3]. Very recently, a high power picosecond Tm^{3+} doped all-fiber oscillator was demonstrated by employing optical fiber Bragg grating for pulse spectrum formation to achieve ultrashort pulse[4-8], which greatly broaden their applications in optical field.

In the previous researches of materials, the Tm^{3+} doped oxide single crystals were mainly focused because of their ordered rigid crystal lattice, higher chemical-physical stability as well as the advantage of direct diode pumping at ~800 nm[9-10]. Generally, oxide single crystals inherit low transmission in mid-infrared range, low luminescent efficiency and high matrix phonon energy, which limits their practical application in optical devices. Actually, the fluoride single crystal is more beneficial to be as 2.0 μm laser due to its high transparency in infrared range, long lifetime of rare earth ions and high luminous efficiency.

Very lately, the α-$NaYF_4$ single crystal doped with Tm^{3+} was successfully fabricated using KF as flux[11]. However, the growth of single crystal with big size and high quality becomes more difficulty due to the use of KF flux. The FK composition may introduce into the α-$NaYF_4$ single crystal as defects of impurities. $Na_5Lu_9F_{32}$ is a kind of fluoride compounds with excellent optical properties[12]. Our recent investigation showed that the characteristic absorption band at 2.7 μm of OH^{-1} almost disappeared in $Na_5Lu_9F_{32}$ single crystal, it indicated that the $Na_5Lu_9F_{32}$ single crystal possesses very lower OH^{-1} content which is very important to eliminate the non-radiative energy transfer from the excited state of Tm^{3+} ion to OH^{-1}[13]. Moreover, a more homogeneous distribution of Tm^{3+} ion in the $Na_5Lu_9F_{32}$ single crystal can be expected because the difference of ionic radii between Tm^{3+} (0.87Å) and Lu^{3+} (0.85Å) is closer than that between Tm^{3+} and Y^{3+} (0.893Å). Thus, a higher optical quality of Tm^{3+} doped $Na_5Lu_9F_{32}$ single crystal is proposed for the intense emission at 1.8 μm. However, there are almost no reports on Tm^{3+} doped $Na_5Lu_9F_{32}$ single crystal for 2 μm laser.

Toward this end, Tm^{3+} doped $Na_5Lu_9F_{32}$ single crystals were grown. Typical performance of 2 μm emission spectra and an optimum doping concentration have been investigated in this study.

1 Experiments

An improved Bridgman method was used for growth of the Tm^{3+} doped $Na_5Lu_9F_{32}$ single crystals. The NaF, LuF_3 and TmF_3 raw materials with high purity of 99.999% were purchased from the market. The molar ratio of NaF : LuF_3 : TmF_3 is 50 : 50-χ : χ (χ=0.5, 1, 1.5, 2, 4). The initial powders were mixed richly for 1 h. The detailed growing process has already reported elsewhere[14].

The polished slices with various Tm^{3+} doped concentrations were transparent as shown in Fig.1. The X-Ray Diffraction (XRD) was recorded by using a XD-98X diffractometer (XD-3, Beijing). The real Tm^{3+} concentrations in single crystal were measured by an inductively coupled plasma atomic emission spectroscopy (ICP-AES PerkinElmerInc, Optima 3 000). Table 1 lists the measured Tm^{3+} concentrations and the molar fractions of Tm^{3+} in raw material. A Cary 5 000 UV/VIS/NIR spectrophotometer was used for measurement of the absorption spectra. The emission spectra were recorded under the 790 nm LD excitation by a Triax 320 type spectrometer. The fluorescence lifetime at 1.86 μm were recorded with FLSP920 fluorescence spectrophotometer. All these measurements were carried out at room temperature.

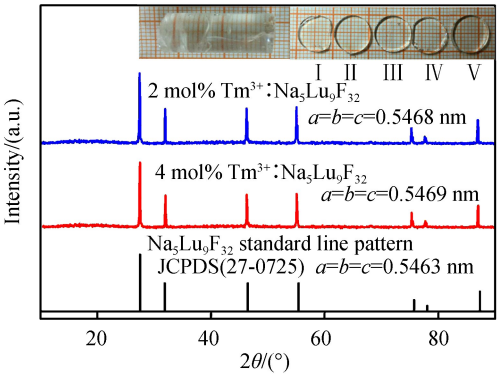

Fig.1 XRD pattern of 2.0 mol% and 4.0 mol% Tm^{3+} doped $Ma_5Lu_9F_{32}$ and the $Na_5Lu_9F_{32}$ stadard line pattern

Table 1 Measured Tm^{3+} concentrations in single crystals and molar fractions of Tm^{3+} in starting material

Samples	Ⅰ	Ⅱ	Ⅲ	Ⅳ	Ⅴ
Tm^{3+}/mol%	0.5 mol%	1.0 mol%	1.5 mol%	2.0 mol%	4.0 mol%
10^{20} N/cm^3	1.25	2.52	3.76	5.03	10.06

2 Results and discussion

Fig.1 shows the X-ray diffraction pattern of 2.0 mol% and 4.0 mol% Tm^{3+} doped $Na_5Lu_9F_{32}$ and the $Na_5Lu_9F_{32}$ standard line pattern. The other Tm^{3+} doped samples also exhibit similar XRD characteristics. Compared with peak positions of JCPDS cards (27-0725) of $Na_5Lu_9F_{32}$ crystal, the measured XRD diffraction peaks and relative intensities are similar to the standard line patterns. The measured XRD patterns strongly indicated that the obtained crystal was pure cubic phase, and the incorporation of Tm^{3+} ions does not give rise to any obvious peak change. The calculated cell parameters for 2mol% and 4mol% Tm^{3+} doped $Na_5Lu_9F_{32}$ crystal are $a=b=c=0.546\ 8$ nm and $a=b=c=0.546\ 9$ nm. The lattice parameter of the single crystal is tended to become big as increase of Tm^{3+} doping concentration because the radius size of Tm^{3+} is slightly bigger than that of Lu^{3+}. It suggests that Tm^{3+} ion substitutes for Lu^{3+} site in $Na_5Lu_9F_{32}$ crystal because of the same valence state and similar ionic radius.

Fig.2 illustrates the absorption spectra of various Tm^{3+} doped $Na_5Lu_9F_{32}$ crystals in the wavelength range from 400 nm to 2 200 nm. It can be observed from Fig.2 that the absorption intensities increase gradually with the continuous increase of the Tm^{3+} doping concentration from 0.5 mol% to 4.0 mol%, while the positions of the peaks remain unchanged. According to the Dieke energy level diagram, six absorption bands located at 463, 656, 680, 782, 1 208 and 1 684 nm can be attributed to the transitions from the ground state $^3H_6$ to the excited states $^1G_4$, $^3F_2$, $^3F_3$, $^3H_4$, $^3H_5$ and $^3F_4$ of Tm^{3+} ion.

Fig.3 presents the emission spectra of different Tm^{3+} doped $Na_5Lu_9F_{32}$ crystals from 1 100 to 2 200 nm wavelength measured exciting of 790 nm LD at room temperature. In these emission spectra, there are two fluorescence emission peaks at around 1.49 μm (relatively weak) and 1.86 μm, which are related to Tm^{3+} transitions $^3H_4\rightarrow{}^3F_4$ and $^3F_4\rightarrow{}^3H_6$, respectively. The relationship between the fluorescence intensity at 1 860 nm and the concentration of the doped Tm^{3+} ions is also shown in the insert of Fig.3. It is clear that the beginning fluorescence emission intensity at 1 860 nm is gradually increasing with the doping concentration of Tm^{3+} increased from 0.5 mo% to 2.0 mol%, then begins to drop dramatically when the concentration continues to rise from 2.0 mol% to 4.0 mol%. It can be noted that there appears a very low intensity at 1.49 μm in low 0.5 mol% Tm^{3+} doping concentration, and it enhances as the increase of Tm^{3+} concentration from 0.5 mol% to 1.0 mol%. The emission band at 1.49 μm almost disappears as Tm^{3+} concentration further increase from 1.0 mol% to 4.0 mol%. This apparent relationship between doped concentration and the values of emission intensity at both 1.49 μm and 1.86 μm is vividly reflected in Fig.3.

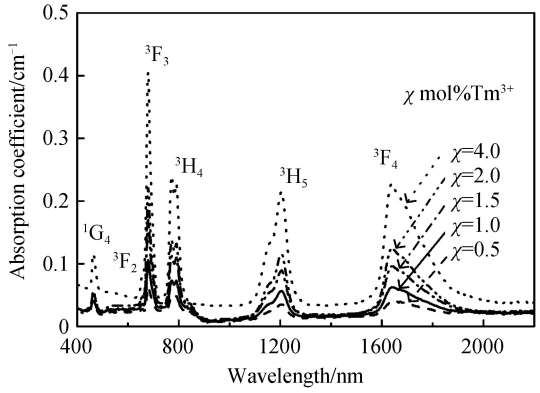

Fig.2 Absorption spectra of Tm^{3+} : $Na_5Lu_9F_{32}$ with various concentrations

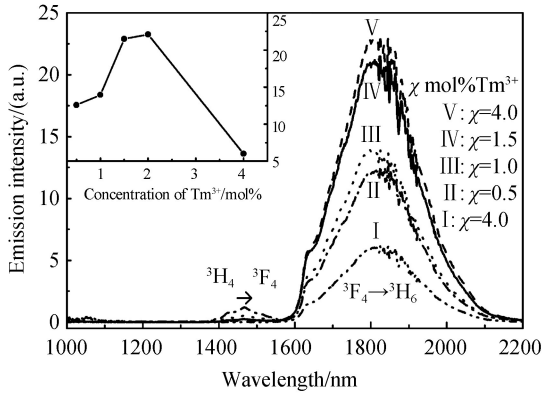

Fig.3 Emission spectra of the Tm^{3+} : $Na_5Lu_9F_{32}$. The inset shows the relationship between Tm^{3+} concentration and emission intensity at 1.86 μm

The possible mechanisms of energy transfer processes between Tm^{3+} ions have been reported in previous work[15-16]. Here we attempt to quantitatively describe the energy transfers between Tm^{3+} ions.

The schematic energy-level diagram for the Tm^{3+} doped $Na_5Lu_9F_{32}$ single crystal is shown in Fig.4. Under the excitation of 790 nm LD, Tm^{3+} transition from the ground state $^3H_6$ to the excited state $^3H_4$, and then Tm^{3+} ion at $^3H_4$ level can open up two energy transfer channels to lower levels. On one respect, Tm^{3+} ions at $^3H_4$ state radiatively transfer to $^3F_4$ level with the 1.49 μm emission, Actually, owing to the energy distance between the $^3H_4$ to $^3F_4$ level (is about 6 909 cm^{-1}) and the $^3F_4$ to $^3H_6$ level (is about 6 105 cm^{-1}) is rather close, the Tm^{3+} ions at $^3H_4$ level easily transition to $^3F_4$ manifold without radiation. As shown in the Fig. 3, the fluorescence intensity of $^3H_4 \rightarrow {}^3F_4$ transition at 1 490 nm is much weaker than that of $^3F_4 \rightarrow {}^3H_6$ transition at 1 860 nm. On the other hand, it can transfer its part of energy to neighbouring Tm^{3+} ions at ground state $^3H_6$ and then new ions enter into $^3F_4$ state. This process was defined as cross-relaxation energy transfer ($^3H_6+{}^3H_4 \rightarrow {}^3F_4+{}^3F_4$) and presented in Fig.4. Finally, two Tm^{3+} ions are excited to $^3F_4$ level. This CR process could result into the stronger 1.86 μm emission, which is well corresponding to the obtained emission spectra. The CR energy transfer becomes higher as increase of the Tm^{3+} ions in crystals. Whereas, a large doping concentration results into concentration quenching which reduces the emission intensity at 1.8 μm as shown in Fig.3 when the doping concentration increases to 4 mol%. Thus, an optimum doping concentration should be obtained. In this experiment, when the doping concentration increase to 1.5 mol%, the CR energy transfer rate gets large enough that most Tm^{3+} ions at $^3H_4$ state would non-radiatively decay to $^3F_4$ sate rather than radiatively decay to $^3H_4$ state by emitting 1.49 μm. It is reason why the emission band at 1.49 μm almost disappears as Tm^{3+} concentration further increase from 1.0 mol% to 4.0 mol%[17]. The measured spectra indicates that the optimum Tm^{3+} doping concentration for realizing maximum emission intensity at 1.86 μm is around 2.0 mol%.

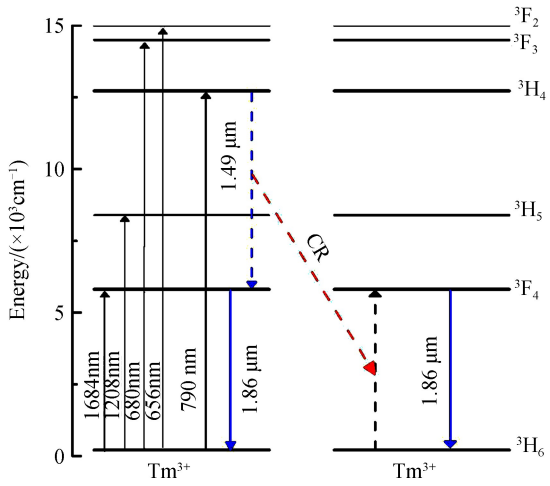

Fig.4 Energy transfer and cross relaxation diagram of Tm^{3+} ions

The fluorescence decay curves for $^3F_4 \rightarrow {}^3H_6$ transition of Tm^{3+} at 1 860 nm excited by 790 nm LD are measured. Fig.5(a) presents the fluorescence decay curves of the $^3F_4$ level for the $Na_5Lu_9F_{32}$ crystals with different Tm^{3+} concentrations. The fluorescence lifetimes were obtained from the decay curves. It is discovered that as the Tm^{3+} concentration increases the fluorescence lifetime decreases in Fig.5(b). In one aspect, the decrease of fluorescence lifetime could be caused by the enhanced nonradiative relaxation, nevertheless in the present case the nonradiative relaxation of $^3F_4$ level will not change since the energy distance between $^3F_4$ and $^3H_4$ does not change and the fluorescence lifetimes were measured at the same temperature. In the other aspect, the decrease of fluorescence lifetime could evoked by energy transfer originated from $^3F_4$ level. In this case, the dependence of fluorescence lifetime on the doping concentration obeys Dexter theory in which it presented as $\tau = \frac{\tau_0}{1+(c/c_0)^{s/3}}$. Here in this equation, τ_0 and c_0 are the intrinsic lifetime and critical concentration of luminescence centers, τ stands for the lifetime when the doping concentration is c. The function $y = \frac{a}{1+(x/b)^c}$ with the same form as the equation was fit to the data in Fig.5 (b), and it can be found that the data can well be fitted by the Dexter theory. In the fitting the process the free parameters′ values with uncertainties were obtained and marked in Fig.5(b). This results tell us that there must be some quenchers which accept the energy from Tm^{3+} at $^3F_4$ and cause the decrease of $^3F_4$ fluorescence lifetime. The quenchers could probably be the unintended dopants or defects in the crystals. The luminous efficiency η plays an important role in the practical application of crystals. It is well known that the luminescence quantum efficiency of Tm^{3+} ion is jointly decided by the radiative lifetime τ_{rad} and fluorescence lifetimes τ. The τ_{rad} = 10.642 ms for 1.0 mol% can be calculated by the J-O

theory according to the measured absorption spectra and chemical-physical properties. The estimated quantum efficiency η for 1.0 mol% is 100.02%.

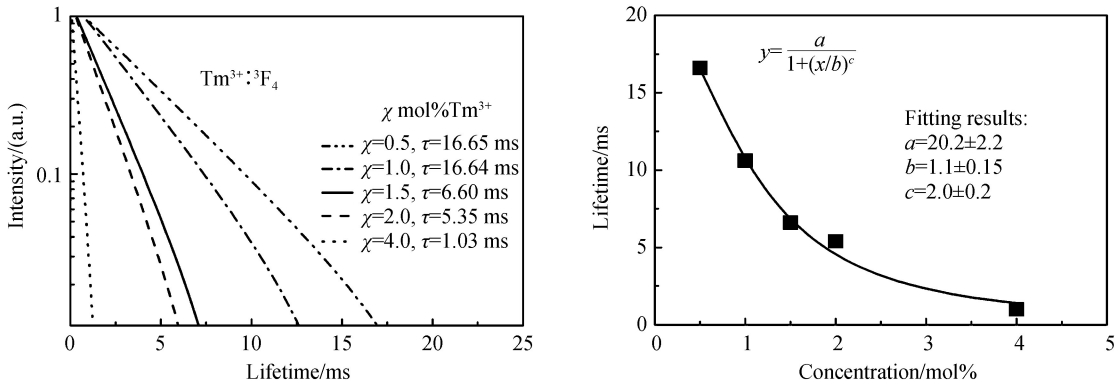

(a) Fluorescence decay curves of the $^3F_4$ level of Tm^{3+}:$Na_5Lu_9F_{32}$ (b) Dependence of $^3F_4$ lifetime of Tm^{3+} concentration

Fig.5 The fluorescence decay spectra for $^3F_4 \rightarrow {}^3H_6$ transition

The stimulated emission cross section is one of the vital parameters to assess the performance of a laser crystal. The absorption cross section (σ_{abs}) can be estimated from the absorption spectrum of Tm^{3+} doped $Na_5Lu_9F_{32}$ single crystal by using following equation.

$$\sigma_{abs(\lambda)} = \frac{2.303OD(\lambda)}{NL} \tag{1}$$

where N is the number of Tm^{3+} ion per unit volume(cm^{-3}), $OD(\lambda)$ is the optical density as a function of wavelength λ, and L is the thickness of the sample, λ is the wavelength.

The stimulated emission cross section (σ_{em}) of Tm^{3+} from $^3F_4 \rightarrow {}^3H_6$ transition can be calculated by McCumber theory [18] as

$$\sigma_{em}(\lambda) = \sigma_{abs}(\lambda)\frac{Z_l}{Z_u}\exp\left(\frac{E_{zl}-h\nu}{kT}\right) \tag{2}$$

where T is temperature (here is the room temperature), k is the Boltzmann constant (1.38×10^{-23} J/K). h is Planck constant, λ is the transition wavelength, Z_l and Z_u is the partition functions between the lower and upper levels respectively, E_{zl} represent the zero line energy, and the E_{zl} value of the $^3F_4$ to $^3H_6$ transition is 5 609 cm^{-1}. The calculated absorption transiting from $^3H_6$ to $^3F_4$ and emission from $^3F_4$ to $^3H_6$ cross sections for 2.0 mol% Tm^{3+} doped $Na_5Lu_9F_{32}$ single crystal are shown in Fig. 6. The maximum value of emission cross section at 1 860 nm is 0.80×10^{-20} cm^2. It should be noticed that the self - absorption is involved into the emission spectrum because the slice of single crystal is usually not thin enough[19].

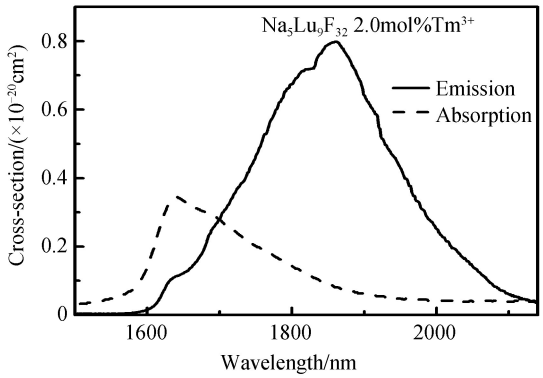

Fig.6 Absorption and Emission cross sections for 1.86 μm in Tm^{3+} : $Na_5Lu_9F_{32}$ crystal

3 Conclusions

Our experiment demonstrated that Bridgman method is a favorable way to grow Tm^{3+} doped $Na_5Lu_9F_{32}$ single crystals. The maximum emission intensity at 1.86 μm can be reached when the doping concentration of Tm^{3+} is 2.0 mol%. At this doping level, the maximum emission cross section at 1.86 μm is calculated to 0.80×10^{-20} cm^2. The measured maximum fluorescent lifetime at 1.86 μm is 16.65 ms. These excellent spectral parameters of Tm^{3+} doped $Na_5Lu_9F_{32}$ single crystals indicated that it may be a potential material for 2 μm laser.

References

[1] STOEPPLER G, PARISI D, TONELLI M, *et al*. High-efficiency 1.9 μm Tm^{3+} : $LiLuF_4$ thin-disk laser[J]. *Optics Letters*, 2012, **37**(7): 1163-1165.

[2] YU Hao-hai, PETROV V, GRIEBNER U, *et al*. Compact passively Q-switched diode-pumped Tm : $LiLuF_4$ laser with 1.26 μm output energy[J]. *Optics Letters*, 2012, **37**(13): 2544-2546.

[3] SHENG Qi-guo, XIA Hai-ping, TANG Qing-yang, *et al*. The optical properties of Tm^{3+} doped $Na_5Lu_9F_{32}$ single crystal [J]. *Optoelectronics Letters*, 2017, **13**(3):201-205.

[4] WANG Ya-zhou, LI Jian-feng, HAN-Lian, *et al*. Q-switched Tm^{3+}-doped fiber laser with a micro-fiber based black phosphorus saturable absorber[J]. *Laser Physics*, 2016, **26**(6): 065104.

[5] CANBAZ F, YORULMAZ I, SENNAROGLU A. Kerr-lens mode-locked 2.3 μm Tm^{3+} : YLF laser as a source of femtosecond pulses in the mid-infrared[J]. *Optics Letters*, 2017, **42**(19): 3964-3967.

[6] MORRIS J, STEVENSON N K, BOOKEY H T. 1.9 μm waveguide laser fabricated by ultrafast laser inscription in Tm : Lu_2O_3 ceramic[J]. *Optics Express*, 2017, **25**(13): 14910-14917.

[7] ZHOU Wei, FAN Xu-liang, XUE Hao, *et al*. Stable passively harmonic mode-locking dissipative pulses in 2 μm solid-state laser[J]. *Optics Express*, 2017, **25**(3): 1815.

[8] REN Xi-kui, DU Chen-lin, LI Chun-bo, *et al*. Silicon wafer: a direct output coupler in Tm : YLF laser[J]. *Chinese Physics Letters*, 2016, **33**(11): 114203.

[9] PENG Ya-pei, YUAN Xin-qiang, ZHANG Jun-jie, *et al*. The effect of La_2O_3 in Tm^{3+}-doped germanate-tellurite glasses for~2 μm emission[J]. *Scientific Reports*, 2014, **4**(17): 5256-5256.

[10] JACKSON S. Cross relaxation and energy transfer upconversion processes relevant to the functioning of 2 μm Tm^{3+}-doped silica fibre lasers[J]. *Optics Communications*, 2004, **230**(1): 197-203.

[11] YANG Shuo, XIA Hai-ping, JIANG Yong-zhang, *et al*. Tm^{3+} doped α-$NaYF_4$ single crystal for 2 μm laser application [J]. *Journal of Alloys and Compounds*, 2015, **643**:1-6.

[12] RUICHAN L, YANG Piao-ping, DAI Yun-lu, *et al*. Lutecium fluoride hollow mesoporous spheres withenhanced up-conversion luminescent bioimaging and light-triggered drug release by gold nanocrystals[J]. *ACS Applied Materials & Interfaces*, 2014, **6**(17): 15550.

[13] WALSH B M, BARNES N P, REICHLE D J, *et al*. Optical properties of Tm^{3+} ions in alkali germanate glass[J]. *Journal of Non-Crystalline Solids*, 2006, **352**(50-51): 5344-5352.

[14] WANG Cheng, XIA Hai-ping, FENG Zhi-gang, *et al*. Infrared luminescent properties of $Na_5Lu_9F_{32}$ single crystals co-doped Er^{3+}/Yb^{3+} grown by Bridgman method[J] *Journal of Alloys and Compounds*, 2016, **686**: 816-822.

[15] XIA Hai-ping, LIN Qiong-fei, ZHANG Jian-li, *et al*. 2 μm mid-infrared optical spectra of Tm^{3+} doped germanium gallate glasses[J]. *Journal of Rare Earths*, 2009, **27**(5): 781-785.

[16] YIN Bing, YANG Zhong-min, YANG Gang-feng, *et al*. The influence of cross-relaxation to the 1.8 μm emission of Tm^{3+} in tellurite Glass[J]. *Rare Metal Materials and Engineering*, 2008, **37**: 85.

[17] WU Jian-feng, JIANG Shi-bin, LUO Tao, *et al*. Efficient thulium-doped 2 μm germanate fiber laser[J]. *IEEE Photonics Technology Letters*. 2006, **18**(2): 334-336.

[18] MINISCALCO W J, QUIMBY R S. General procedure for the analysis of Er^{3+} cross sections[J]. *Optics Letters*, 1991, **16**(4):258.

[19] WEI Yao-wei. Growth and spectroscopic properties of Tm^{3+} doped $LiLa(MoO_4)_2$ crystal[D]. Fuzhou: Fujian institute of research on the structure, Chinese Academy of Sciences, 2009.